Characterization of drivers maintaining atrial fibrillation; correlation with markers of rapidity and organization on spectral analysis

Honarbakhsh S* MRCP BSc, Schilling RJ* FRCP FESC MD, Providencia R* MD, Keating E* BAppSc IBHRE CCDS, Chow A* FRCP MD, Sporton S* FRCP MD, Lowe MD* FRCP MD, Earley MJ* FRCP MD, Lambiase PD* FRCP PhD, Hunter RJ* FESC PhD.

*Barts Heart Centre, St Bartholomew's Hospital, Barts Health NHS Trust, Department of Arrhythmia Management, London, United Kingdom

Corresponding Author:

Dr Ross J Hunter FESC PhD

Electrophysiology Consultant

Barts Heart Centre

Barts Health NHS Trust

W. Smithfield

EC1A 7BE

Email: ross.hunter@bartshealth.nhs.uk

ABSTRACT

Background:

The mechanistic role of localized drivers in persistent atrial fibrillation (AF) remains uncertain. Characteristics of these drivers remains to be established.

Methods:

Patients undergoing catheter ablation for persistent AF were included. The CARTOFINDER mapping system was used to identify drivers with rotational or focal activity. The effect of ablation on drivers identified post-PV isolation was assessed and the correlation to sites of fastest cycle length (CL), highest dominant frequency (DF) and greatest organization using lowest CL variability and highest regularity index (RI) as surrogates. Drivers temporal stability and recurrence rate were assessed and the effect of PV isolation evaluated.

Results:

Thirty patients were included with 154 CARTOFINDER maps created. Potential drivers were mapped in 29/30 patients. Forty-four potential drivers were identified with a pre-defined ablation response in 39 (89%): 23 rotational and 16 focal. The drivers demonstrated spatial stability with temporal periodicity with no driver demonstrating a consecutive repetition of >6 cycles. CL stability correlated best to the driver sites (29/39 confirmed drivers, 74%). Fastest CL and highest DF correlated to driver sites whereby the drivers showed greater temporal stability and recurrence rate. Drivers with rotational activity showed a predilection to low voltage zones (74%) whilst focal drivers did not (56%). PV isolation did not impact AF CL or driver site CL, DF, CL variability and RI.

Conclusions:

Drivers were identified in almost all patients in the form of intermittent but repetitive focal or rotational activation patterns. The mechanistic importance of these phenomena was confirmed by ablation response.

Keywords: Atrial fibrillation, Rotors, Dominant frequency, Cycle length, Pulmonary vein isolation

INTRODUCTION

Localized sources in the form of rotors or focal discharges may sustain AF (1-4). Data is conflicting as to whether these drivers are temporally stable (1) or intermittent (2-4).

Optical mapping in sheep has suggested that AF is maintained by high frequency sources and that electrograms recorded at these sites have rapid cycle length (CL) and a high dominant frequency (DF) (5, 6). Mapping studies in humans have identified sites with high DF (7-9). Pulmonary vein (PV) isolation and linear ablation has shown to reduce global left atrial (LA) DF (9, 10). In one study ablation at sites of high DF resulted in CL prolongation or AF termination (11). However, others have argued that the lack of spatiotemporal stability of DF sites suggests that they cannot represent sites of stable drivers (12, 13).

Better characterization of drivers in the human LA may facilitate their identification using sequential mapping. Our group and others have recently reported mapping AF drivers using the CARTOFINDER system (3). We sought to characterize drivers in detail and study their relationship with electrogram characteristics in the time and frequency domain.

METHODS

Patients undergoing catheter ablation for persistent AF (<24 months and no previous AF ablation) were prospectively included. All procedures were performed with un-interrupted anticoagulation therapy and intravenous heparin administration to achieve an ACT of 300-350ms. The procedures were performed either under conscious sedation or general anesthesia. Patients provided informed consent for their involvement in this

study, and the study was approved by the UK National Research Ethics Service (16/LO/1379) and complies with declaration of Helsinki. The study was registered on clinicaltrials.gov as a sub-study of an ongoing trial (NCT02950844).

i) Electrophysiological mapping

Mapping was performed with CARTOFINDER (CARTO, Biosense Webster, Inc, CA) (3). LA geometry and a high-density bipolar voltage map were created using a PentaRay® NAV catheter with 2-6-2mm electrode spacing (Biosense Webster, Inc, CA). Points that were ≥3mm from the geometry surface were filtered as not being in contact with the myocardium, and points were respiratory gated. To collect the wavefront maps, a 50mm or 60mm 64-pole basket catheter was used to record unipolar signals (Constellation, Boston Scientific, Natick, MA and FIRMap Abbott, CA, USA). The catheter was sized from the LA diameters obtained from a transthoracic echocardiogram performed on the day of the procedure as advised by the manufacturer. A decapolar catheter (Biosense Webster, Inc, CA) was positioned in the coronary sinus (CS). A Thermocool© SmartTouch™ or Thermocool© SmartTouch Surround Flow™ catheter (Biosense Webster, Inc, CA) was used for ablation. The basket catheter was positioned in the LA through an 8Fr Mullen's (Cook Medical, In, USA) or 8.5Fr SL1 sheath (Daig Medical, MN).

All patients had wide area circumferential ablation to achieve PV isolation. Pre and post-PV isolation all patients had a minimum of two CARTOFINDER maps created with the basket catheter repositioned between recordings. The post-PV isolation maps guided further ablation in the LA. This was commenced 20min post-PV isolation to eliminate any delayed effect of PV isolation on CL prolongation during ablation in the

LA body. Plausible AF drives were defined as ≥1.5 360 degrees rotations or ≥2 focal discharges with radial spread (3). Driver sites were ablated and a confirmed driver was defined as one whereby ablation resulted in i) slowing of CL ≥30ms ii) organization to AT iii) termination to sinus rhythm (3). The electrogram characteristics at the confirmed driver sites were reviewed offline.

ii) Ablation strategy at driver site

The ablation strategy used in this study has been described previously (3). In brief a lesion was delivered at the center of the driver site with further ablation surrounding the initial lesion in a cluster, avoiding the creation of linear lesions. Ablation was stopped once the study pre-defined ablation response was achieved, no residual signal identified at the ablation site or >5min of ablation had been performed. Beyond isolating PVs and targeting potential drivers no additional ablation was performed in AF. If the AF organized into an AT this was mapped and ablated.

iii) Driver characteristics

For each driver three characteristics were evaluated: reproducibility, recurrence and temporal stability. Reproducibility was defined as the number of CARTOFINDER maps in each patient that showed the same confirmed driver. The number of times a confirmed driver was identified and met the study definition of driver during a 30-second recording was defined as the recurrence rate. Temporal stability was defined as the number of consecutive repetitions identified during each occurrence of a driver.

iv) CLs

Using the CARTOFINDER system CL was measured as the time difference between

two consecutive atrial signal annotations on the unipolar signals recorded from the basket catheter. From this the 'dominant CL' for each electrode pole was determined over a 30-second recording. The dominant CL for each electrode was defined using a CL histogram, plotting CL on the x axis and the number of cycles on the y axis, whereby the dominant CL is the center of the narrowest range of CLs in the histogram containing 50% of the cycles (14). The dominant CL at each pole was then reviewed firstly as a CL map on the anatomical geometry with the colors projected varying depending on the underlying CL thereby allowing sites with the faster dominant CL to be identified. This was also reviewed quantitatively whereby the dominant CL obtained at each electrode pole was compared to identify the electrode(s) with the faster dominant CLs. The position of these poles was then identified on the anatomical geometry. The site or sites with the fastest dominant CL were thereby identified and their relationship to sites of confirmed drivers were evaluated.

v) DF

To determine DF, following filtering of far field ventricular signals, a Butterworth 2nd order filter was applied to the unipolar signals. Rectification was then performed to take the absolute value of the signal followed by applying a low pass filter to the signal (20Hz Butterworth 2nd order). Spectral analysis was then performed using a combination of periodogram multiplied by a Hamming window and a Welch periodogram to estimate the power spectral density and DF. Four-second windows were used with 50% overlap between the windows. The DF was then determined for each four-second window and the median of these values was taken as the DF for the 30-second recording. This was performed for all the basket electrodes that were in contact

and recorded unipolar signals. The DF for each electrode is then compared with each other to identify the site of highest DF.

Using the DF data obtained, 3D DF maps were created which were superimposed on the anatomical maps created in CARTO. Correlation between sites of highest DF and confirmed driver sites was assessed. This was examined quantitatively by determining the DF at each electrode and identifying the sites of highest DF in the LA. Again this was correlated to sites of confirmed AF drivers.

To evaluate the accuracy and utility of these DF and CL calculations, the sites of highest DF were compared to sites of fastest CLs to determine the level of correlation between these two parameters. If these parameters were meaningful it would be expected that these two parameters should effectively correlate with each other.

vi) CL variability (CLV) and regularity index (RI)

Two markers for organization were used; RI and CLV. The correlation between sites of greatest organization and confirmed drivers were assessed. RI was used to assess the spread of frequencies at each electrode over a 30-second recording. RI for each electrode was calculated as the ratio of the power at the DF and its adjacent frequencies for that electrode to the power of the 2.5 to 20-Hz band for each 4-second window with the median of these values taken as the RI. Thereby sites of higher RI therefore denote less frequency variation. Again sites of highest RI were compared to sites of confirmed drivers.

The CLV was determined for each pole through taking the standard deviation (SD) of the CLs in relation to the dominant CL for that electrode pole. This was also reviewed as a CLV map and compared to sites of confirmed drivers.

A driver was said to co-locate with sites of fastest CL, highest DF, lowest CLV or highest RI if the center of the driver was ≤1cm from these sites. The fastest CL, highest DF and highest RI were defined as the CL, DF and RI within the top decile. The lowest CLV was defined as a CLV in the bottom decile.

vii) Bipolar voltage

Areas with a bipolar voltage of <0.5mV were defined as low voltage zones (LVZs) (15). Voltage maps were divided into non-LVZs (nLVZs) and LVZs. Sites of confirmed AF drivers were then categorized as existing in either a nLVZ or LVZ.

vi) CFAEs

CFAEs were defined as fractionated activity (defined as continuous deflections without pause at the isoelectric line for ≥70ms) occupying ≥70% of a 2.5 second sample (16). Using a custom written script in Matlab (Mathworks, MA, USA) sites of CFAEs meeting the above definition were identified on the LA geometry. The correlation between these sites and sites of confirmed drivers were evaluated.

Statistical analysis

All statistical analyses were performed using SPSS (IBM SPSS Statistics, Version 24 IBM Corp, NY, USA). Continuous variables are displayed as mean ± SD or median (IQR). Categorical variables are presented as a number and percentage. The student t-

test, or its non-parametric equivalent, Mann-Whitney U test when appropriate was used for comparison of continuous variables. Fisher's exact test was used for the comparison of nominal variables. ROC curves were performed to determine the diagnostic ability of LVZs in predicting the presence of rotational drivers. A p-value of <0.05 was considered significant.

RESULTS

Thirty patients were prospectively included in this study. The baseline demographics are in Table 1. In one of the 30 patients the post-PV isolation CARTOFINDER maps were generated with inappropriate annotation of atrial signals due to excessive noise on many of the unipolar electrograms due to damage to the basket. This patient was therefore excluded from much of the analysis, leaving 29 patients for analysis of post-PV isolation maps.

All procedures were performed successfully without any complications. The average procedure duration was 264.0±62.5 min and median fluoroscopy time of 2.8min (IQR 0-3.1min). The total ablation time following PV isolation until reaching the study endpoint (AF termination or CL slowing ≥30ms) was 3.3±0.7min. The mean LA coverage achieved was 72.1±15.4%. The average number of bipolar voltage points taken was 812±134.

i) Potential drivers on CARTOFINDER maps pre and post-PV isolation

The number of potential drivers identified pre and post-PV isolation is shown in Figure 1. In the 30 patients, 154 CARTOFINDER maps were created (5.3±1.3 maps per

patient) out of which 76 were created pre-PV isolation (2.6±0.7 maps per patient) and 78 post-PV isolation (2.7±0.7 maps per patient).

Forty-four potential drivers were identified in the 29 patients with post-PV isolation maps (1.6±0.8 drivers per patient). Twenty-two of these 44 potential drivers in 19 patients were identified on the pre-PV isolation maps (22/44, 50%). No additional drivers were seen on the pre-PV isolation maps that were not seen on the post-PV isolation. The maps that did not demonstrate potential driver(s) showed a combination of multiple broad linear wavefronts which circulated seemingly randomly, and sites of disorganized activity with no clear discernable wavefront which was more common in pre-PV isolation maps (25/76, 33% vs. 12/79, 15%). A majority of patients had had only 1 potential driver identified on pre-PV isolation (16/19 patients, 84%) and post-PV isolation maps (18/29, 62%) (Figure 1).

The anatomical location and characteristics of the potential drivers identified on post-PV isolation maps is demonstrated in Table 2 and Figure 2. The potential drivers were most frequently mapped to the anterior wall (14/44, 31.8%) of which a majority were rotational drivers (42.9% focal and 57.1% rotational drivers). Following this, the roof was the next most common site drivers were mapped to (10/44, 22.7%), of which rotational drivers were most common (70% rotational and 30% focal drivers). Overall, of the 44 potential drivers identified on the post-PV isolation maps, 26 were rotational (59%) and 18 were focal with radial spread (41%). On the pre-PV isolation maps there was an equal distribution of rotational and focal drivers (11/22, 50% rotational and 11/22, 50% focal).

In those patients that had drivers identified on pre-PV isolation maps the AF CL at the LA appendage was slower than those that did not have drivers identified (171.8±19.6ms vs. 141.2±28.0ms; p=0.03). Further to this, mean CLV was lower in those with drivers identified compared to those that did not have drivers identified on the pre-PV isolation maps (35.6±5.3ms vs. 41.5±5.5ms; p=0.017). There was no significant difference in driver temporal stability with drivers seen pre and post-PV isolation compared to those seen only post-PV isolation (3.3±0.9 vs. 2.9±0.8; p=0.13).

ii) Ablation response at the potential driver sites

Ablation at the 44 potential driver sites resulted in an effect that met the study criteria, for a confirmed driver in 39 instances. The 5 potential driver sites where no response to ablation was observed were identified in patients that had other potential drivers mapped. All 29 patients had a confirmed driver identified (1.3±0.6 confirmed driver per patient). Out of the 39 confirmed drivers 23 (59%) were rotational and 16 (41%) were focal.

Ablation at the 39 confirmed driver sites resulted in AF termination with 20 of the drivers (51.3%, 20 out of 29 patients (69%)). In the remaining 19 confirmed drivers ablation resulted in slowing of the CL ≥30ms. Drivers that were also identified on the pre-PV isolation maps were more commonly associated with AF termination compared to drivers only identified post-PV isolation (13/18, 72.2% AF termination vs. 3/14, 21.4%; p=0.001).

iii) Reproducibility, temporal stability and recurrence of confirmed drivers

The confirmed drivers were shown to be reproducible with an average of 77.9±19.4% of maps in each patient demonstrating the same confirmed driver. All confirmed drivers were spatially conserved but were intermittent. During a 30-second recording each driver occurred 8.7±5.4 times (the recurrence rate). During each occurrence a driver completed 3.1±0.9 consecutive repetitions (the temporal stability). The maximum number of consecutive repetitions was 6 for a focal driver and 4.5 for a rotational driver (Figure 3).

Focal drivers were more temporally stable in that they complete a greater number of consecutive repetitions than rotational drivers (3.4±0.9 vs. 2.9±0.8; p=0.07). Focal drivers also had a higher recurrence rate than rotational drivers (11.9±6.2 vs. 6.3±3.3; p=0.001). However, there was no significant difference in AF termination rates between these two drivers (8/16, 50% focal vs. 12/23, 52% rotational; p=1.00). However, when reviewing all drivers, those that resulted in AF termination showed greater temporal stability than those that did not (3.4±0.9 vs. 2.7±0.6; p=0.001).

iv) CL and DF

Of the 154 CARTOFINDER maps the site of fastest CL was the same as the site of highest DF in 147/154 maps (95.5%).

v) CLV and RI

Reviewing all 154 CARTOFINDER maps, sites of lowest CLV correlated to sites of highest RI on majority of the maps (148/154, 96.1%).

v) CL, DF, CLV and RI and their correlation with confirmed driver sites

Table 3 demonstrates the correlation of each confirmed driver site with fastest CL, highest DF, lowest CLV and highest RI. It also shows the relationship of the confirmed driver sites with bipolar voltage and sites of CFAE.

Table 4 demonstrates the correlation between confirmed driver sites and fastest CL, highest DF, lowest CLV and highest RI on a per driver and patient basis. Sites of confirmed drivers correlated less frequently to sites of fastest CL and highest DF compared to sites of lowest CLV and highest RI, whereby 28 (71.8%) and 26 (66.7%) of confirmed drivers correlated to these sites respectively.

Drivers correlating with sites of fastest CL had greater temporal stability (3.5±0.9 vs. 2.8±0.6 consecutive repetitions; $p<0.002$) and higher recurrence rate (13.3±4.8 vs. 4.8±1.0 occurrences per 30 second recording; $p<0.001$) than drivers not correlating to these sites. Similarly, drivers correlating with sites of highest DF also showed greater temporal stability (3.6±1.0 vs. 2.8±0.6; $p<0.001$) and higher recurrence rate (14.5±3.7 vs. 5.1±2.0; $p<0.001$). This suggests that the correlation with fastest CL and highest DF site is dependent on the temporal stability of the driver. As focal drivers had greater temporal stability and higher recurrence rate they also correlated more frequently to sites of highest DF (10/16, 63% vs. 5/23, 22%; $p=0.018$) and fastest CL (10/16, 63% vs. 7/23, 30%; $p=0.059$) compared to rotational drivers. Figure 4A-C demonstrates a focal driver site correlating to the site of lowest CLV and highest DF.

On a per patient basis, sites of fastest CL and highest DF correlated to at least one driver in 13 (45%) and 11 out of 29 patients (38%) respectively. The lowest CLV site

correlated to a driver site in 25 out of 29 patients (86%). The site of highest RI correlated to a confirmed driver site in 21 out of 29 patients (72%).

Drivers that correlated with sites of lowest CLV (20/28 vs. 0/11, $p<0.001$) and higher RI (20/26 vs. 1/12, $p<0.001$) were associated with higher rates of AF termination.

vi) Bipolar voltage and confirmed driver sites

Out of the 39 confirmed drivers identified, a majority was mapped to LVZs (26/39, 67%). Whilst rotational drivers demonstrated a predilection for LVZs (17/23, 74% LVZs vs. 6/23, 26% non-LVZs) focal drivers did not (9/16, 56% LVZs vs. 7/16, 44% non-LVZs). However, this difference in characteristics between rotational and focal drivers did not reach significance (17/23 vs. 9/16, $p=0.31$). A greater proportion of LVZs was however predictive of the presence of rotational drivers on mapping with a sensitivity of 92.9% and specificity of 77.8% respectively with an optimal cutoff of 49% (AUC 0.93, 95% CI 0.82-1.00; $p=0.001$).

vii) CFAE and confirmed driver sites

Thirty sites of CFAEs meeting study criteria were identified in 25 patients which include 35 confirmed drivers (86% of patients, 1.03±0.56 CFAE sites per patient). CFAEs were seen to predominantly involve the anterior wall including anterior LA appendage and anteroseptum (50%) followed by posterior wall (23%), lateral wall including antero and posterolateral (17%) and roof (10%). Out of the 30 CFAE sites, 14 correlated to sites of confirmed drivers (47%) and 14 of the 35 confirmed drivers corresponded to CFAE sites (40%). Out of the 35 confirmed drivers, CFAE sites correlated to 40% of rotational driver sites (8/20) and 40% of focal driver sites (6/15).

On a per patient basis, a CFAE site correlated to a site of at least one confirmed driver in 13 out of the 25 patients (52%).

viii) Effect of PV-isolation on driver characteristics

PV isolation did not impact on any of the driver characteristics assessed (Table 5). The temporal stability and recurrence of confirmed drivers pre and post-PV isolation was not significantly different (Table 5). CL, DF, CLV and RI were also unchanged (Table 5). Further to this, post-PV isolation there was no significant difference in the LA appendage CL when compared to the pre-PV isolation LA appendage CL (141±28ms pre-PVI vs. 145±26ms post-PVI; p=0.68).

DISCUSSION

Targeting localized drivers with either rotational or focal activity results in AF termination in a large proportion of patients. All drivers identified pre-PV isolation were also identified post-PV isolation with no discernible change in their CL or DF suggesting that these drivers are independent of the PVs. Ablation of drivers that were (a) identified both pre- and post PV isolation, (b) more temporally stable, or (c) showed greater organization on spectral analysis (lower CLV and higher RI) were associated with a higher rate of AF termination, suggesting greater mechanistic importance. Drivers with a rotational pattern of activation had a predilection for LVZs with a greater proportion of LVZs being predictive of the presence of rotational drivers. Focal drivers did not show a predilection for LVZs. Confirmed driver sites correlated effectively with sites of AF organization measured using CLV or RI whereas correlation with sites of greater rapidity measured using faster CL and higher DF was less robust and was dependent on driver temporal stability and recurrence rate.

i) Characterization of drivers and response to ablation

Ablation at a majority of the potential drivers sites identified produced a positive response (89%), with AF termination for more than half of the drivers. Drivers with greater temporal stability were more likely to be associated with AF termination.

Approximately 60% of identified drivers had rotational activation and 40% were focal. Drivers with rotational activation had a predilection for LVZs whereas focal drivers did not. The confirmed drivers mapped in this study were spatially conserved but with temporal periodicity. The temporal stability of the drivers were variable but no driver completed >6 consecutive repetitions. The intermittent nature of the localized drivers is more in line with the data obtained using the ECGi system (2) than that reported with the TOPERA system (1). Focal drivers were shown to have a greater temporal stability and higher recurrence rate compared to drivers with rotational activity; however, there was no significant difference in the AF termination rates with ablation of these two driver types. This suggests that they are similarly important in maintaining AF.

Drivers seen pre- and post-PV isolation were more commonly associated with AF termination on ablation compared to drivers only seen post-PV isolation. Those with drivers identified on pre-PV isolation maps had slower LA appendage CL and lower average CL variability indicating more organized AF.

The lack of impact of PV isolation on several driver characteristics suggests that these drivers are independent of the PVs. The response to ablation seen at the driver sites contrasts with the lack of impact on AF CL with PV isolation. This arguably suggests

that although the PVs may play an important role in AF initiation, they may be less important for the maintenance of AF than the drivers identified in this study.

ii) CL, DF, CLV and RI and their correlation with confirmed driver sites

Small non-randomized studies have shown that targeting sites of highest DF have been associated with CL prolongation during ablation of persistent AF (11) and have shown promising long-term success (17). However, others have argued that the lack of spatiotemporal stability of DF sites suggests that they cannot represent sites of stable drivers (12, 13).

It is noteworthy that some studies have highlighted a lack of correlation between DF and CL regardless of whether unipolar or bipolar signals were analyzed or whether the QRS was subtracted (18, 19). One potential flaw of fast fourier transform (FFT) is that it makes the assumption that the signal is 'stationary' (i.e. consistent) which is not the case in AF. The signal obtained during AF will be subject to phase shift. If a long time window is set for the FFT analysis this phase shift can result in the FFT analysis either failing to pick up the change in frequencies or represent these as noise which will impact the DFs obtained. If however, a shorter time window is used, the extent of phase shift will be minimized as there is less likely to be great variation in the signal over a short time window and as a result less impact on the DFs obtained during the FFT analysis. The CARTOFINDER system records a 30-second sample, but uses short 4-second windows for analysis with 50% overlap between windows to overcome this 'stationary challenge'. Using this system we demonstrated a strong correlation between sites of highest DF and fastest CLs. The closer correlation observed with this methodology is biologically plausible and suggests a more meaningful result.

To date no study has mapped drivers in the human LA to allow direct comparison to sites of rapid CL, high DF or markers of organization. These data demonstrate that overall there was a moderate correlation between drivers and sites of rapid CL or highest DF. However, this correlation may depend on driver temporal stability and recurrence. Drivers that showed greater temporal stability and higher recurrence rates correlated to sites of highest DF and fastest CL, whereas drivers that were less temporally stable or recurred less often did not. Nevertheless, these data do not suggest that mapping of AF using DF or fastest CL is likely to be reliable in detecting drivers.

Increased overall organization in AF has shown to be associated with termination of AF with flecainide (20) or ablation (21). Prospectively targeting sites with increased organization index, derived from DF has resulted in regional AF organization (22). In this study we used two markers for organization based on signal analysis in both the time and frequency domains: CLV and RI. These parameters correlated well with each other and with sites of confirmed drivers. Unlike CL and DF, the correlation seen was consistent unconditional of the characteristics of the drivers. This is compatible with data from computer modeling studies showing that sites of increased organization as evidenced by a high organization index correlates better with the location of drivers than peaks in DF (23). These data suggest that CLV and RI are likely to be more useful for detecting drivers than CL or DF.

iii) *CFAE and driver sites*

CFAE ablation remains controversial. We utilized a custom algorithm to identify electrograms that had continuous fractionation for >70% of the sample, since this is

compatible with what others have predicted at rotor sites (5, 6) and has been shown to correlate with CL prolongation during ablation (15, 24). However, less than half of CFAE sites corresponded to drivers and less than half of drivers corresponded to CFAE. This is compatible with findings by others (25). Taken together these data suggest that CFAE are unlikely to be reliable in identifying drivers.

Limitations

In this study we focused on electrophysiological end points to determine the mechanistic significance of potential drivers. CL prolongation was one of these endpoints and its importance is less clear than AF termination. However, CL prolongation has been utilized by others (3, 18, 26) and the CL slowing of ≥30ms used to define a positive response is the most stringent definition used to date. Furthermore, if only the drivers resulting in AF termination were considered significant the results would be very similar albeit with fewer drivers.

Although drivers are spatially conserved these data suggest temporal periodicity. However, it is possible that this represents intermittent failure to detect drivers perhaps due to electrogram fractionation (27).

CONCLUSIONS

Utilizing this novel mapping system we successfully identified localized LA drivers in all patients. AF termination or substantial CL slowing occurred with ablation of both focal and rotational drivers, suggesting that they are important in maintaining AF. Ablation of drivers with greater temporal stability was more likely to cause AF termination. Electrogram analysis in the time and frequency domains showed that

drivers corresponded to sites of greater electrogram organization (lower CLV and higher RI) but not markers of rapidity (high CL and DF). Randomized studies are needed to test the clinical utility of these parameters in guiding ablation for AF.

FUNDING

A Project Grant from the British Heart Foundation (Grant number: PG/16/10/32016) funded this work.

DISCLOSURES

Prof. Schilling has received speaker and travel grants from Biosense Webster and research grants from Biosense Webster and Boston Scientific. Dr Hunter has received travel grants for the purposes of attending conferences from Biosense Webster and Medtronic. Prof Lambiase receives educational and research grants from Boston Scientific.

REFERENCES

1. Narayan SM, Krummen DE, Shivkumar K, Clopton P, Rappel WJ, Miller JM. Treatment of Atrial Fibrillation by the Ablation of Localized Sources: CONFIRM (Conventional Ablation for Atrial Fibrillation With or Without Focal Impulse and Rotor Modulation) Trial. J Am Coll Cardiol 2012;60:628-36.
2. Haissaguerre M, Hocini M, Denis A, et al. Drivers domains in persistent atrial fibrillation. Circulation 2014; 130:530-8.
3. Honarbakhsh S, Schilling RJ, Dhillon G, et al. A novel mapping system for panoramic mapping of the left atrium: application to detect and characterize localized sources maintaining AF. JACC Clin Electrophysiol. 2017 Published online first.
4. Benharash P, Buch E, Frank P, Share M, Tung R, Shivkumar K, Mandapati R. Quantitative analysis of localized sources identified by focal impulse and roter modulation mapping in atrial fibrillation. Circ Arrhythm Electrophysiol. 2015;8:554-61.
5. Skanes AC, Mandapati R, Berenfeld O, Davidenko JM, Jalife J. Spatiotemporal periodicity during atrial fibrillation in the isolated sheep heart. Circulation. 1998;98:1236 –1248.
6. Mandapati R, Skanes AC, Chen J, Berenfeld O, Jalife J. Stable microreentrant sources as a mechanism of atrial fibrillation in the isolated sheep heart. Circulation. 2000;101:194 –199.
7. Lin YJ, Tai CT, Kao T, Tso HW, Higa S, Tsao HM, Chang SL, Hsieh MH, Chen SA. Frequency analysis in different types of paraoxysmal atrial fibrillation. J Am Coll Cardiol. 2006;47:1401-7.
8. Stiles MK, Brooks AG, Kuklik P, John B, Dimitri H, Lau DH, Wilson L, Dhar

S, Roberts-Thomson RL, Mackenzie L, Young GD, Sanders P. High-density mapping of atrial fibrillation in humans: relationship between high-frequency activation and electrogram fractionation. J Cardiovasc Electrophysiol. 2008;19:1245-53.

9. Nakahara S, Toratani N, Nakamura H, Higashi A, Takayanagi K. Spatial relationship between high-dominant frequency sites and the liner ablation line in persistent atrial fibrillation: its impact on complex fractionated electrograms. Europace 2013; 15:189-197.
10. Tuan J, Jeilan M, Kundu S, Nicolson W, Chung I, Stafford PJ, Ng GA. Regional fractionation and dominant frequency in persistent atrial fibrillation: effects of left atrial ablation and evidence of spatial relationship. Europace 2011;13:1550-1556.
11. Sanders P, Berenfeld O, Hocini M, Jais P, Valdyanathan R, Hsu LF, Garrigue S, Takahashi Y, Rotter M, Sacher F, Scavee C, Ploutz-Snyder R, Jalife J, Haissaguerre M. Spectral analysis identifies sites of high-frequency activity maintaining atrial fibrillation in humans. Circulation 2005;112:789-797.
12. Jarman JW, Wong T, Kojodjojo P, Spohr H, Davies JE, Roughton M, Francis DP, Kanagaratnam P, Markides V, Davies DW, Peters NS. Spatiotemporal behavior of high dominant frequency during paroxysmal and persistent atrial fibrillation in the human left atrium. Circ Arrhythm Electrophysiol. 2012;5:650-8.
13. Habel N, Znojkiewicz P, Thompson N, Muller JG, Mason B, Calame J, Calame S, Sharma S, Mirchandani G, Janks D, Bates J, Noori A, Karnbach A, Lustgarten DL, Sobel BE, Spector P. The temporal variability of dominant frequency and complex fractionated atrial electrograms constrains the validity

of sequential mapping in human atrial fibrillation. Heart Rhythm 2010;7:586-93.

14. Houben RPM, de Grot NMS, Lindemans FW, Allessie MA. Automatic mapping of human atrial fibrillation by template matching. Heart Rhythm 2006;3:1221–1228.
15. Sanders P, Morton JB, Davidson NC, Spence SJ, Vohra JK, Sparks PB, Kalman JM. Electrical remodelling of the atria in congestive heart failure: electrophysiological and electroanatomic mapping in humans. Circulation 2003;108:1461-8.
16. Hunter RJ, Diab I, Tayebjee M, Richmond L, Sporton S, Earley MJ, Schilling RJ. Characterization of fractionated atrial electrograms critical for maintenance of atrial fibrillation: a randomized, controlled trial of ablation strategies (the CFAE AF trial). Circ Arrhythm Electrophysiol. 2011;4:622-9.
17. Yoshida K, Chugh A, Good E, et al. A critical decrease in dominant frequency and clinical outcome after catheter ablation of persistent atrial fibrillation. Heart Rhythm 2010; 7:295-302.
18. Elvan A, Linnenbank AC, van Bemmel MW, Bamdat Misier AR, Delnoy PP, Beukema WP, de Bakker JMT. Dominant frequency of atrial fibrillation correlates poorly with atrial fibrillation cycle length. Circulation 2009;2:634-644.
19. Singh SM, Heist EK, Koruth JS, Barrett CD, Ruskin JN, Mansour MC. The relationship between electrogram cycle length and dominant frequency in patients with persistent atrial fibrillation. J Cardiovasc Electrophysiol. 2009:20:1336-42.

20. Tuan J, Osman F, Jeilan M, Kundu S, Mantravadi R, Stafford PJ, Ng GA. Increase in organization index predicts atrial fibrillation termination with flecainide post-ablation:spectral analysis of intracardiac electrograms. Europace 2010;12:488-93.
21. Takahashi Y, Sanders P, Jais P, Hocini M, Dubois R, Rotter M, Rostock T, Nalliah CJ, Sacher F, Clementy J, Haissaguerre M. Organization of frequency spectra of atrial fibrillation: relevance to radiofrequency catheter ablation. J Cardiovasc Electrophysiol. 2006;17:382-8.
22. Jarman JWE, Wong T, Kojodjojo P, Spohr H, Davies JER, Roughton M, Francis DP, Kanagaratnam P, O'Neil MD, Markides V, Davies DW, Peters NS. Organizational Index mapping to identify focal sources during persistent atrial fibrillation. J Cardiovasc Electrophysiol 25;335-363.
23. Tobon C, Rodriguez JF, Ferrero Jr JM, Hornero F, Saiz J. Dominant frequency and organization index maps in a realistic three-dimensional computational model of atrial fibrillation. Europace 2012;14:v25-v32.
24. Takahashi Y, O'Neill MD, Hocini M, Dubois R, Matsuo S, Knecht S, Mahapatra S, Lim KT, Jais P, Jonsson A, Sacher F, Sanders P, Rostock T, Bordachar P, Clementy J, Klein GJ, Haissaguerre M. Characterization of electrograms associated with termination of chronic atrial fibrillation by catheter ablation. J Am Coll Cardiol. 2008;51:1003-1010.
25. Narayan SM, Shivkumar K, Krummen DE, Miller JM, Rappel WJ. Panoramic electrophysiological mapping but not electrogram morphology identified stable sources for human atrial fibrillation: stable atrial fibrillation rotors and focal sources relate poorly to fractionated electrograms. Circ Arrhythm Electrophysiol. 2013;6:58-67.

26. Haissaguerre M, Lim KT, Jacquemet V, et al. Atrial fibrillatory cycle length: a computer stimulation and potential clinical importance. Europace 2007;9:vi64-70.

27. Atienza F, Calvo D, Almendral J, et al. Mechanisms of fractionated electrograms formation in the posterior left atrium during paroxysmal atrial fibrillation in humans. J Am Coll Cardiol. 2011;57:1081-1092.

Table 1- Demonstrates the baseline characteristics of the cohort

Baseline characteristics	**Cohort n=30**
Age years mean ± SD	64±10
Male n (%)	19 (63)
Diabetes mellitus n (%)	0
Hypertension n (%)	8 (27)
TIA/CVA* n (%)	2 (7)
Ischemic heart disease n (%)	2 (7)
Cardiac surgery n (%)	1 (3)
Left ventricular EF† ≥ 55% n (%)	21 (70)
LA area cm^2 mean ± SD	27.3±6.3
Bipolar voltage mV mean ± SD	0.39±0.17
AF duration months, mean ± SD	17.5±6.2
Previous AT ablation (including AT and AF patients) n (%)	
Cavo-tricuspid isthmus-dependent flutter	4 (15)
Focal or micro-reentrant	2 (7)
Current medical strategy	
Beta-blockers including Sotalol	20 (67)
Amiodarone	7 (23)
Flecainide	4 (13)
Current anticoagulation strategy	
Warfarin	8 (27)
Noval oral anticoagulation	22 (73)

*TIA/CVA- transient ischemic attack/cerebrovascular attack

†EF- Ejection fraction

Table 2- Demonstrates

the characteristics of the potential AF drivers mapped with the CARTOFINDER system and the response to ablation at the driver site

Patient ID	Driver type	Driver location in LA	Proportion of maps with driver %	Visible on pre-PV maps	Ablation response	Ablation duration m
1	Focal	Posterior/inferior lateral	100	Yes	AT	2.8
2	Rotational	Anterior	67	No	Nil	1.8
	Focal	Lateral	67	Yes	Sinus	3.2
3	Rotational	Posterior LAA*/lateral	100	No	SCL	2.4
4	Focal	Roof/LAA	50	Yes	SCL	3.7
	Focal	Posterior/inferior lateral	50	Yes	AT	4.2
5	Focal	Mid Anterior	100	Yes	SCL	4.8
	Rotational	Posterior/inferior lateral	100	Yes	AT	3.7
6	Rotational	Mid Anterior	75	No	AT	3.3
7	Rotational	Mid Posterior/inferior	100	No	A T	4.1
8	Rotational	Inferior RLPV^{T}/septal	67	Yes	Sinus	3.8
9	Focal	Low Anterior	100	No	SCL	3.5
	Rotational	Mid Roof	100	Yes	Sinus	4.0
10	Rotational	Posterior LAA	75	No	SCL	4.6
11	Rotational	Anteroseptal	100	No	SCL	4.1
12	Rotational	Mid Roof	100	Yes	Sinus	3.4
13	Rotational	Mid Anterior	100	No	SCL	2.8
14	Rotational	Anteroseptal	100	No	SCL	4.1
15	Rotational	Roof/RUPV^{Ŧ}	67	Yes	Nil	3.5
	Focal	Roof/LAA	67	Yes	SCL	2.5
16	Rotational	Roof	100	Yes	SCL	4.1
17	Focal	Anterior LAA	100	Yes	Sinus	2.2
18	Rotational	Mid Roof	67	Yes	AT	2.7

19	Focal	Lateral	67	No	Nil	3.5
	Rotational	Anteroseptal	67	No	Nil	3.8
	Rotational	Septal	33	No	SCL	2.7
20	Rotational	Septal	50	No	AT	2.5
21	Rotational	Low Anterior	75	Yes	SCL	2.7
22	Focal	Septal	67	No	SCL	2.7
	Focal	Posterior Roof	67	Yes	AT	3.3
23	Focal	Anterior LAA	67	Yes	Sinus	3.4
24	Rotational	Mid Roof	50	No	Sinus	2.7
25	Rotational	Low Posterior/inferior	75	Yes	Sinus	3.2
26	Focal	Posterior/inferior	33	No	Nil	3.1
	Rotational	Inferior RUPV/septal	67	No	SCL	2.5
	Rotational	Mid Roof	67	No	SCL	2.9
	Focal	Mid Anterior	67	Yes	AT	2.8
27	Focal	Lateral	100	No	SCL	2.8
	Rotational	Mid Anterior	67	Yes	Sinus	2.8
28	Focal	Anterior LAA	67	No	SCL	3.4
	Rotational	Septal	67	No	SCL	4.1
	Focal	Lateral	100	Yes	AT	3.1
29	Focal	Proximal CS[^]	67	No	SCL	2.2
	Rotational	Lateral	67	Yes	Sinus	1.9

[*]LAA- Left atrial appendage

[Ŧ]RLPV- Right lower pulmonary vein

[Ŧ]RUPV- Right upper pulmonary vein

[^]CS- Coronary sinus

Table 3- Demonstrates the characteristics of the confirmed drivers and their relationship with CL, DF, CLV, RI, bipolar voltage and sites of CFAE. Highest RI, Fastest CL and peak DF refers to the top decile. Lowest CLV refers to the lowest decile.

Patient ID	Driver type	Consecutive repeats in 30 sec mean ± SD	Recurrence in 30sec mean ± SD	Correlation with					
				Lowest CLV*	Highest RI[T]	Fastest CL[T]	Peak DF^	CFAE§	Voltage zone
1	Focal	2.3±0.6	5.2±0.6	Yes	Yes	No	No	No	nLVZ
2	Focal	4.0±0.8	7.5±0.7	Yes	Yes	No	No	No	nLVZ
3	Rotational	2.3±0.6	4.5±0.8	No	No	No	No	No	LVZ
4	Focal*	2.3±0.6	14.5±0.7	Yes	Yes	Yes	Yes	Yes	LVZ
	Focal*	4.0±2.7	16.5±0.7	Yes	Yes	Yes	Yes	Yes	nLVZ
5	Focal*	2.3±0.6	16.2±0.9	Yes	Yes	Yes	Yes	Yes	LVZ
	Rotational	2.8±0.4	6.3±0.6	Yes	Yes	No	No	No	LVZ
6	Rotational*	2.2±0.7	13.7±1.5	Yes	Yes	Yes	Yes	Yes	LVZ
7	Rotational	4.0±0.0	4.5±0.7	Yes	Yes	No	Yes	Yes	LVZ
8	Rotational	3.0±0.8	4.2±0.6	Yes	Yes	No	No	No	nLVZ
9	Focal	2.8±1.0	4.0±0.0	No	No	No	Yes	Yes	LVZ
	Rotational*	2.9±1.0	4.0±0.0	Yes	Yes	Yes	No	No	LVZ
10	Rotational	2.3±1.1	3.6±0.9	No	No	No	No	Yes	nLVZ
11	Rotational*	2.5±0.7	12.3±1.1	No	No	Yes	Yes	No	LVZ
12	Rotational	2.3±0.9	3.2±0.8	Yes	Yes	No	No	No	nLVZ
13	Rotational	2.4±0.8	4.3±0.9	No	No	No	No	No	nLVZ
14	Rotational	2.2±0.6	5.2±0.9	No	No	No	No	Yes	LVZ
15	Focal	2.8±0.8	3.5±0.7	No	No	No	No	No	nLVZ
16	Rotational	2.3±0.6	5.2±0.7	Yes	Yes	No	No	N/A	LVZ
17	Focal*	3.0±1.3	12.7±1.5	Yes	Yes	Yes	Yes	Yes	LVZ
18	Rotational	2.8±0.9	5.6±0.3	Yes	Yes	No	No	No	nLVZ
19	Rotational*	3.0±1.3	13.5±1.2	Yes	No	Yes	No	N/A	LVZ

20	Rotational*	3.8±0.6	8.0±0.0	Yes	Yes	Yes	Yes	N/A	LVZ
21	Rotational	2.7±0.1	3.7±0.6	Yes	Yes	No	No	Yes	nLVZ
22	Focal*	3.5±0.7	9.7±2.1	Yes	Yes	Yes	Yes	No	nLVZ
	Focal*	4.3±0.2	14.7±1.5	Yes	Yes	Yes	Yes	No	nLVZ
23	Focal*	5.1±0.1	21.5±2.1	Yes	Yes	Yes	Yes	N/A	LVZ
24	Rotational	2.2±0.3	5.0±0.0	Yes	Yes	No	No	Yes	LVZ
25	Rotational	4.0±0.6	4.7±1.1	Yes	Yes	No	No	No	LVZ
26	Rotational	2.1±0.3	4.0±1.0	No	No	No	No	No	LVZ
	Rotational*	4.8±0.3	10.3±1.2	Yes	Yes	Yes	Yes	No	LVZ
	Focal *	4.8±0.2	18.7±1.5	Yes	Yes	Yes	Yes	Yes	nLVZ
27	Focal	2.8±0.2	5.2±1.2	No	No	No	No	No	nLVZ
	Rotational*	4.5±0.4	12.2±1.3	Yes	Yes	Yes	Yes	Yes	LVZ
28	Focal*	3.5±0.1	18.0 ±0.0	Yes	Yes	Yes	Yes	No	LVZ
	Rotational	2.5±0.1	6.0±1.4	No	No	No	No	No	LVZ
	Focal*	3.8±0.1	18.0±0.0	Yes	Yes	Yes	Yes	No	nLVZ
29	Focal	2.9±0.3	4.3±0.9	No	No	No	No	No	LVZ
	Rotational	3.2±0.2	5.0±0.0	Yes	No	No	No	Yes	LVZ

*CLV- Cycle length variability

ŦRI- Regularity index

ŦCL- Cycle length

^DF- Dominant frequency

§CFAE- Complex fractionated atrial electrograms

Table 4- Demonstrates the correlation between fastest CL, peak DF, lowest CL variability and regularity index at confirmed driver site and at potential driver sites where ablation had no response.

	Confirmed driver sites correlating (out of 39 drivers)	**Patients with at least one confirmed driver correlating (out of 29 patients)**
Fastest CL[*] n (%)	17 (44)	13 (45)
Percentile at driver sites, mean ± SD		15.1±13.6
Highest DF[Ŧ] n (%)	15 (38)	11 (38)
Percentile at driver sites, mean ± SD		18.7±15.4
Lowest CLV[ŦŦ] n (%)	29 (74)	25 (86)
Percentile at driver sites, mean ± SD		7.5±7.9
Highest RI[^] n (%)	26 (67)	21 (72)
Percentile at driver sites, mean ± SD		8.4±8.1

[*]CL- Cycle length

[Ŧ]DF- Dominant frequency

[ŦŦ]CLV- Cycle length variability

[^]RI- Regularity index

Table 5- Demonstrates driver characteristics pre and post-PV isolation and thereby the impact of PV isolation on the drivers

	Pre-PV isolation	Post-PV isolation	p-value
Recurrence in 30 sec, mean ± SD	8.4±4.8	8.6±5.5	0.89
Consecutive repeats in 30 sec mean ± SD	3.0±0.7	3.1±0.9	0.90
CL[*] at the driver site, ms mean ± SD	134.1±19.9	134.1±22.7	0.98
Peak DF[Ŧ] at the driver site, Hz mean ± SD	5.8±0.5	5.7±0.6	0.45
CLV[Ŧ] at the driver site, ms mean ± SD	12.2±5.7	12.9±7.1	0.84
RI[^] at the driver site, Hz mean ± SD	0.4±0.1	0.5±0.1	0.12

[*]CL- Cycle length

[Ŧ]DF- Dominant frequency

[Ŧ]CLV- Cycle length variability

[^]RI- Regularity index

FIGURE LEGEND

Figure 1- Demonstrates a flow chart of the study identifying the number of potential drivers identified pre and post-PV isolation and how many of these were confirmed drivers and what the response was to ablation at these sites.

Figure 2A-B-

Ai-Aii- Shows LA geometry maps in AP (Ai) and PA (Aii) position. The maps show the distribution of the drivers on the anatomical LA surface with the red circles representing rotational drivers and blue circles representing focal drivers.

Bi-Bii- Shows LA geometry maps in AP (Bi) and PA (Bii) position. The maps demonstrates the percentage of the drivers mapped to each anatomical surface. Purple= roof, blue=anterior, red=septal and yellow=posterior. The black circles highlight anteroseptal and posterolateral surfaces.

Figure 3- Bar chart graph that demonstrates the number of consecutive repetitions a confirmed driver showed during each occurrence. The dark grey bars represent a focal driver and the light grey bar represents a rotational driver.

Figure 4A-C-

Ai-iii) CARTOFINDER maps on a LA CARTO geometry in a tilted supine view that demonstrates a focal driver with radial spread along the roof.

B-C) CARTOFINDER maps on a LA CARTO geometry that demonstrates the correlation between site of lowest CL variability (B) and highest DF (C) and the focal driver site.

Figure 1

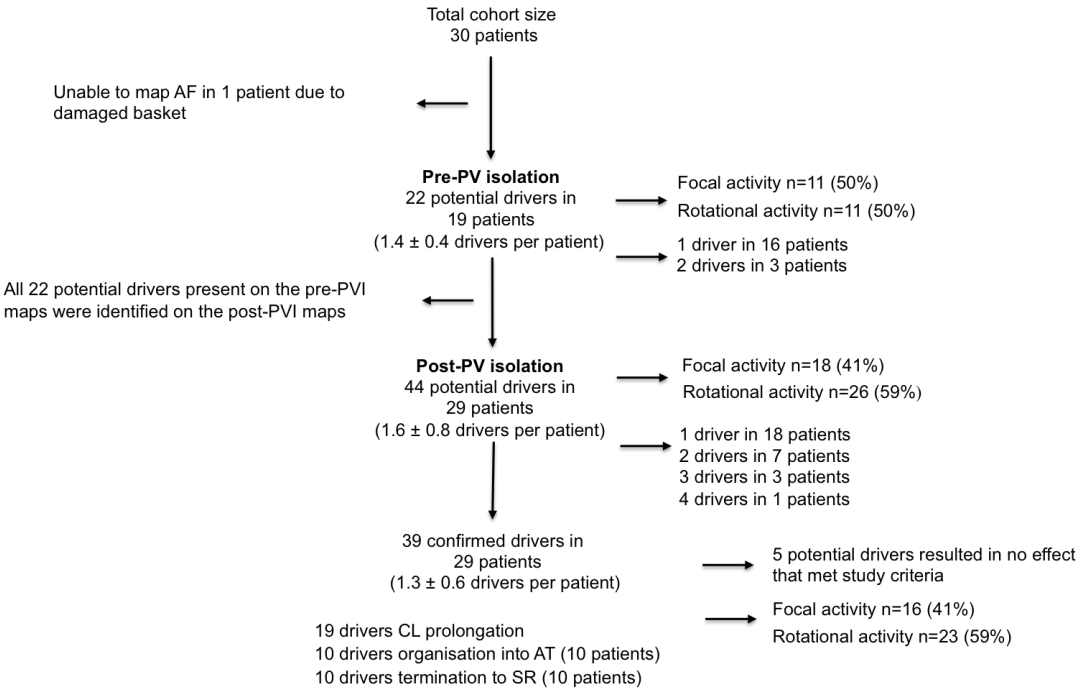
Total cohort size
30 patients
Unable to map AF in 1 patient due to damaged basket
Pre-PV isolation
22 potential drivers in 19 patients
(1.4 ± 0.4 drivers per patient)
Focal activity n=11 (50%)
Rotational activity n=11 (50%)
1 driver in 16 patients
2 drivers in 3 patients
All 22 potential drivers present on the pre-PVI maps were identified on the post-PVI maps
Post-PV isolation
44 potential drivers in 29 patients
(1.6 ± 0.8 drivers per patient)
Focal activity n=18 (41%)
Rotational activity n=26 (59%)
1 driver in 18 patients
2 drivers in 7 patients
3 drivers in 3 patients
4 drivers in 1 patients
39 confirmed drivers in 29 patients
(1.3 ± 0.6 drivers per patient)
5 potential drivers resulted in no effect that met study criteria
Focal activity n=16 (41%)
Rotational activity n=23 (59%)
19 drivers CL prolongation
10 drivers organisation into AT (10 patients)
10 drivers termination to SR (10 patients)

Figure 2A-B

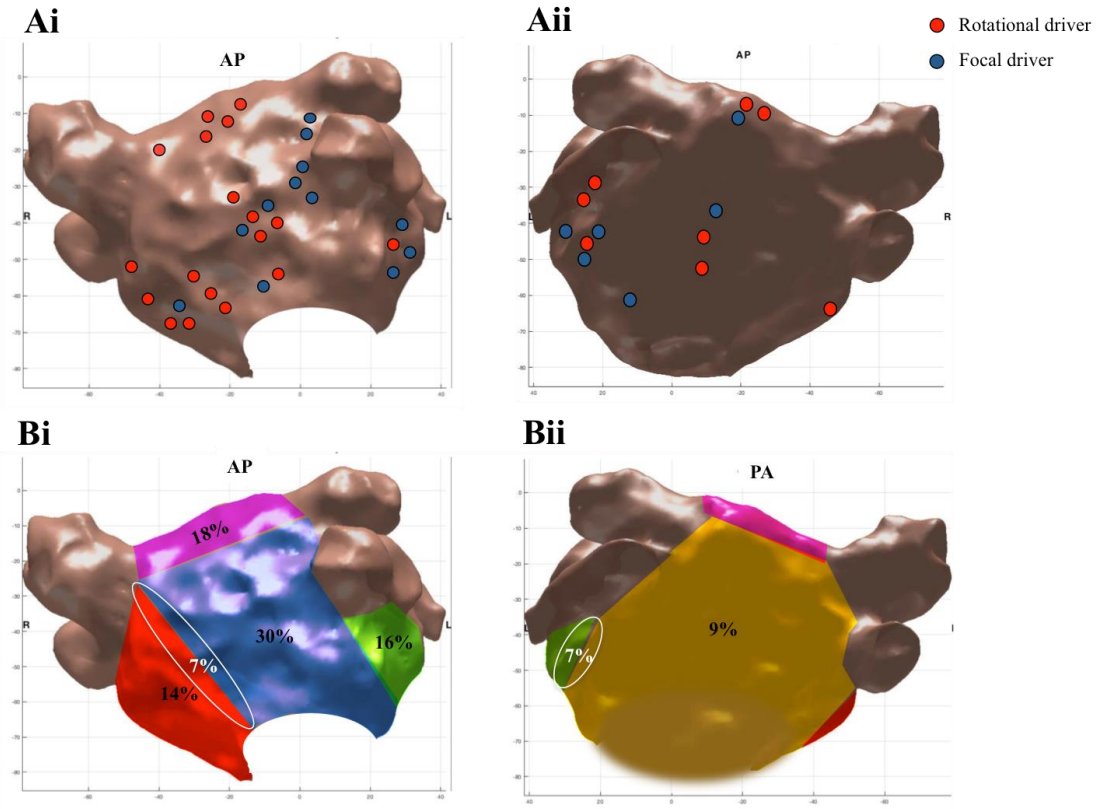
Ai
AP
Aii
AP
Rotational driver
Focal driver
Bi
AP
18%
30%
16%
7%
14%
Bii
PA
9%
7%

Figure 3

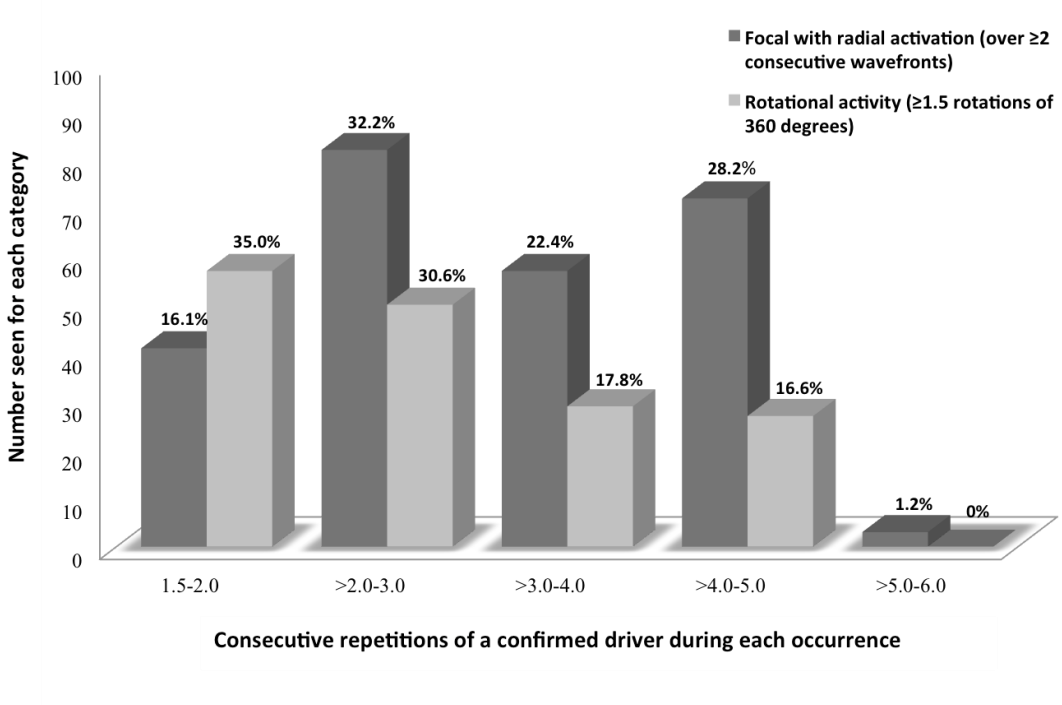
Focal with radial activation (over ≥2 consecutive wavefronts)
Rotational activity (≥1.5 rotations of 360 degrees)
Number seen for each category
100
90
80
70
60
50
40
30
20
10
0
16.1%
35.0%
32.2%
30.6%
22.4%
17.8%
28.2%
16.6%
1.2%
0%
1.5-2.0
>2.0-3.0
>3.0-4.0
>4.0-5.0
>5.0-6.0
Consecutive repetitions of a confirmed driver during each occurrence

Figure 4A-C